

# Ultrafast serrodyne optical frequency translator

Received: 17 June 2022

Accepted: 3 November 2022

Published online: 19 December 2022

 Check for updates

Prannay Balla <sup>1,2,3</sup>, Henrik Tünnemann <sup>1</sup>, Sarper H. Salman<sup>1,2,3</sup>, Mingqi Fan<sup>1</sup>, Skirmantas Alisauskas <sup>1</sup>, Ingmar Hartl <sup>1</sup> & Christoph M. Heyl <sup>1,2,3</sup> 

The serrodyne principle enables an electromagnetic signal to be frequency shifted by applying a linear phase ramp in the time domain. This phenomenon has been exploited to frequency shift signals in the radiofrequency, microwave and optical regions of the electromagnetic spectrum over ranges of up to a few gigahertz, for example, to analyse the Doppler shift of radiofrequency signals for noise suppression and frequency stabilization. Here we employ this principle to shift the centre frequency of high-power femtosecond laser pulses over a range of several terahertz with the help of a nonlinear multi-pass cell. We demonstrate our method experimentally by shifting the central wavelength of a state-of-the-art 75 W frequency comb laser from 1,030 nm to 1,060 nm and to 1,000 nm. Furthermore, we experimentally show that this wavelength-shifting technique supports coherence characteristics at the few hertz-level while improving the temporal pulse quality. The technique is generally applicable to wide parameter ranges and different laser systems, enabling efficient wavelength conversion of high-power lasers to spectral regions beyond the gain bandwidth of available laser platforms.

Ultrafast high-power lasers offer pulses with durations that reach the few-femtosecond range. Following the invention of chirped-pulse amplification (CPA), the past three decades are marked by major advances in ultrafast science and metrology as well as in strong-field physics and material sciences. An important part of this progress can be attributed to advances in ultrafast high peak and/or average power laser technology. High-power lasers opened a path to capture sub-femtosecond electron dynamics<sup>1</sup>, they have enabled great insights into the proton structure<sup>2</sup> and the development of suitable tools for next-generation chip manufacturing via short-wavelength nanolithography<sup>3</sup>. Dedicated laser parameters are required for many innovations and applications, including application-optimized wavelength, intensity, pulse length, beam properties and many more. In particular, the wavelength is a very important yet not very flexible parameter.

Today, ytterbium-, titanium:sapphire- and, recently, thulium-based laser platforms are commonly used for generating femtosecond pulses at high peak and/or average power. Although these laser systems typically operate only at specific wavelengths defined

by the bandwidth of the laser gain medium, modern laser technology provides a variety of options to build wavelength-tunable laser sources. Wavelength-shifting approaches are routinely employed at low power levels using stimulated Raman scattering in optical fibres<sup>4,5</sup>, soliton-shifting methods<sup>6,7</sup>, dispersive wave generation<sup>8,9</sup> and Raman-based shifting schemes in hollow-core fibres or capillaries<sup>10,11</sup>. Wide spectral coverage and ultrashort pulses can also be provided by parametric frequency conversion employed, for example, in optical parametric amplifiers<sup>12</sup>. However, these methods typically suffer from low conversion efficiency or limited power-handling capabilities. By contrast, pulse post-compression technology offers a route to reach ultrashort few-femtosecond pulse duration with high efficiency. In particular, when combined with ytterbium-based lasers, ultrashort pulses with kilowatts of average power<sup>13</sup> that approach the terawatt-peak power regime can be obtained<sup>14</sup>. However, these and other high-peak power laser platforms lack a wavelength-tuning option. Serrodyne frequency-shifting methods—historically learned from radiofrequency technology<sup>15,16</sup> and later on applied to continuous-wave lasers<sup>17–21</sup>—can

<sup>1</sup>Deutsches Elektronen-Synchrotron DESY, Hamburg, Germany. <sup>2</sup>Helmholtz-Institute Jena, Jena, Germany. <sup>3</sup>GSI Helmholtzzentrum für Schwerionenforschung GmbH, Darmstadt, Germany. ✉e-mail: [christoph.heyhl@desy.de](mailto:christoph.heyhl@desy.de)

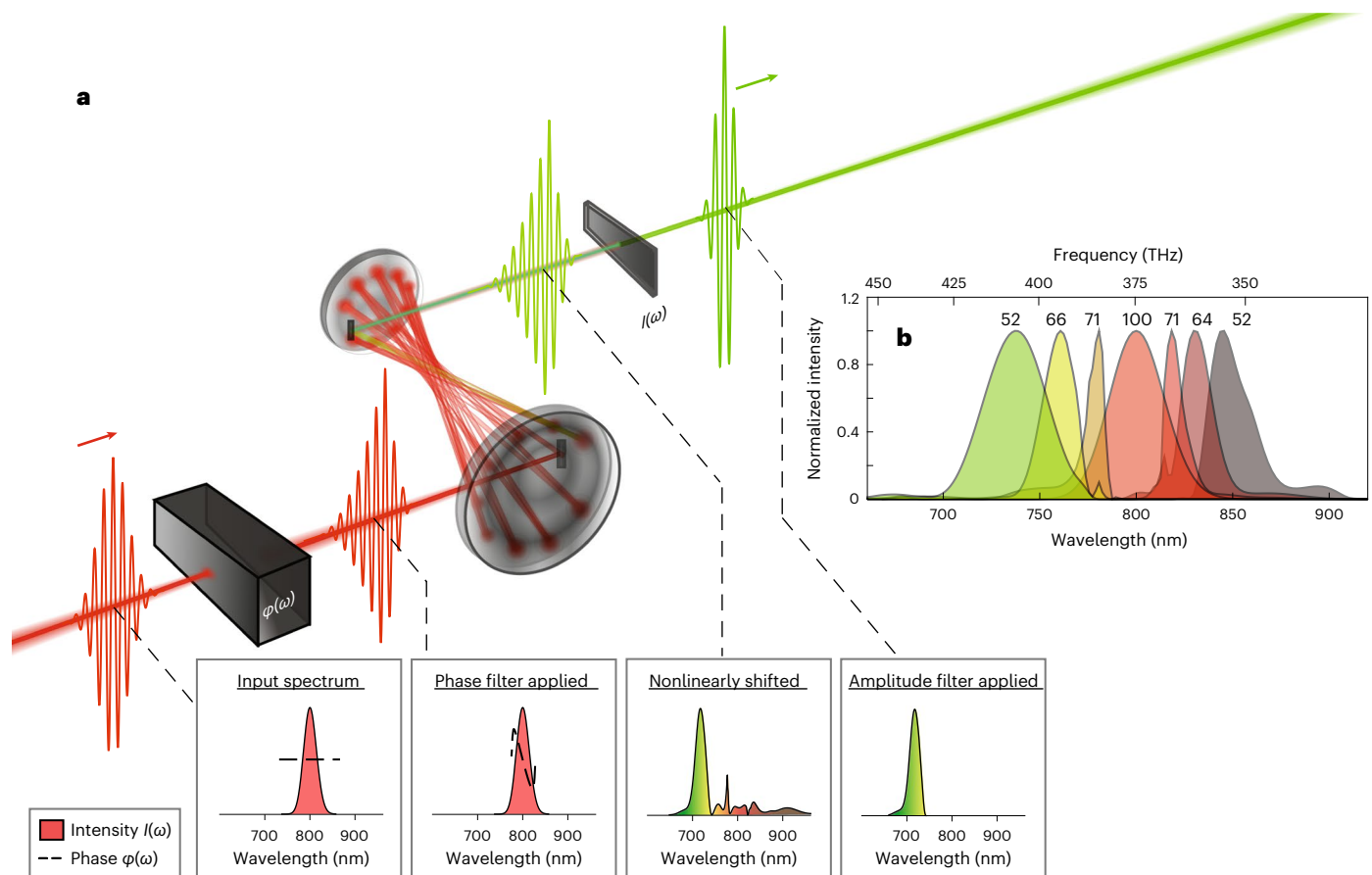


**Fig. 1 | Ultrafast optical serrodyne frequency shifting via self-phase modulation in an MPC. a**, Illustration of the principle: phase ( $\phi(\omega)$ ) and optional amplitude shaping via a wave shaper enables the generation of a temporal saw-tooth pulse, which is sent through a dispersion-balanced nonlinear MPC yielding a frequency-shifted spectrum, which can be filtered using a dichroic filter ( $I(\omega)$ ). The insets display simulations that consider a 40 fs input laser pulse centred at

800 nm and a perfectly dispersion-balanced MPC. **b**, Simulation of the shifting process considering the same input pulses as used in **a** and an MPC made of commercially available broadband matched-pair dielectric mirrors using two mirror bounces between consecutive passes through the focus. The displayed efficiencies (%) correspond to the fractional power of the spectrally filtered signal with respect to the MPC output.

offer a solution to this problem. Translated from continuous-wave signals to ultrashort laser pulses, the method can provide high efficiencies as well as compatibility with terawatt-peak and kilowatt-average powers while supporting key characteristics required for precision metrology applications, including phase coherence and carrier-envelope-offset frequency preservation.

The serrodyne principle states that, for a given signal, the frequency of the signal shifts when a linear phase is applied in the time domain<sup>22</sup>. Such a phase can be applied by, for example, electro-optic modulation<sup>17</sup>. We instead use all-optical methods utilizing the Kerr-effect, which can be employed to transfer a linear amplitude modulation in time into a linear phase ramp. A temporal saw-tooth pulse with centre frequency  $\omega_0$  undergoing self-phase modulation (SPM) gets frequency-shifted to  $\omega = \omega_0 + \Delta\omega$ . The magnitude and direction of the frequency shift are given by:

$$\Delta\omega = -\Phi_{\text{NL}} \frac{dI(t)}{dt}, \quad (1)$$

where  $I(t)$  is the time-dependent laser intensity and  $\Phi_{\text{NL}}$  is the accumulated nonlinear phase, commonly known as the  $B$ -integral. From equation (1), we note that for a larger frequency shift, we can either increase the  $B$ -integral or the intensity gradient by creating a steeper pulse slope. Although the slope steepness is limited by the available spectral bandwidth, large  $B$ -integrals can be acquired by utilizing guiding concepts; however, the temporal pulse shape has to be maintained

for efficient SPM-based spectral shifting, which is typically not the case when SPM and linear dispersion are present. The recent introduction of nonlinear multipass cells (MPCs)<sup>23,24</sup> offers a solution to this challenge, providing the possibility to accomplish dispersion-balanced SPM that supports large  $B$ -integrals, thus enabling simple but very effective multiterahertz frequency shifting<sup>25</sup>.

Our frequency-shifting method is illustrated in Fig. 1a. The phase and, optionally, the amplitude of an ultrashort laser pulse are shaped using a pulse shaper, implemented, for example, using a programmable spatial light modulator. The laser pulse is then spectrally shifted in a second step using a dispersion-balanced MPC. The wavelength-shifted spectrum is then separated from residual broadband wavelength components via a dichroic filter.

We numerically demonstrate our method considering a 40 fs, Fourier-limited input pulse (Gaussian spectrum) as available from standard titanium:sapphire laser systems. Using feed-forward optimization routines (see Methods), we calculate an optimized phase providing maximum efficiency when shifting to a targeted output wavelength. The amplitude shape was not altered. Optimum efficiency is typically reached when the temporal pulse profile approaches a saw-tooth shape. The saw-tooth orientation thereby dictates the spectral shifting directions. Wavelength tuning is possible by simply changing the  $B$ -integral in the MPC and by optimizing the wave-shaper settings. The resulting highly efficient wavelength shifting characteristics simulated under realistic experimental conditions are shown in Fig. 1b. Although our simulations already support a shifting range of over 50 THz with

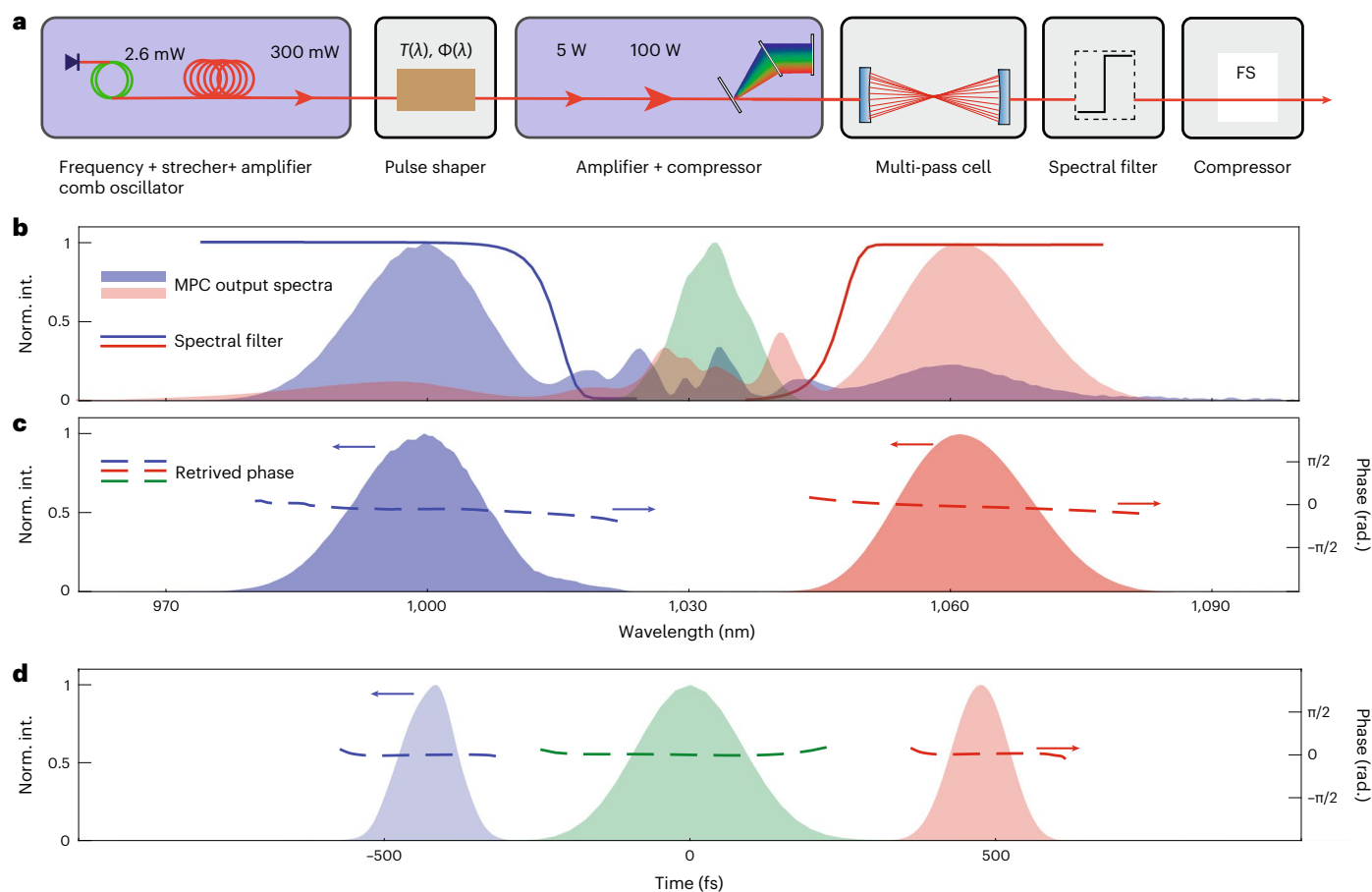


**Fig. 2 | Set-up and spectral shifting results.** **a**, Schematic of the experimental set-up including a high-power frequency comb laser (blue boxes) complemented with pulse shaper, MPC, spectral filter and fused-silica (FS) glass compressor for frequency shifting (grey boxes). **b**, Measured spectrum at the MPC input (green) and at the output shifted to 999 nm (blue) and to 1,062 nm (red) shown together

with the transmission of the spectral filters (solid lines). **c**, Corresponding measured spectra and retrieved phases of the output pulses after spectral filtering and compression. **d**, Corresponding temporal intensity profiles and phases retrieved from second harmonic FROG measurements displayed together with the reconstructed MPC input laser pulse (green).

an efficiency larger than 50%, higher efficiencies and larger frequency ranges can be expected with improved mirror characteristics.

To experimentally demonstrate our frequency-shifting method, we employ a high-power ytterbium-based frequency comb system delivering 200 fs pulses at a 65 MHz repetition rate. A schematic system layout is depicted in Fig. 2. A pulse shaper introduced in the low-power section (340 mW) of a three-stage amplifier chain utilizing CPA is used to introduce a phase optimized to produce a saw-tooth pulse after compression. Again, the amplitude shape was not changed using the shaper. At the CPA output, pulses at an average power of 76 W are coupled into an MPC. The MPC consists of two dielectric concave mirrors with a 100 mm radius of curvature separated by a distance of 187 mm. The dispersion of each mirror is approximately matched to 10.5 nm ultraviolet fused silica within a 980–1,080 nm bandwidth, corresponding to multiple anti-reflection coated windows inserted into the MPC. The MPC is operated with 32 roundtrips yielding an overall transmission of 81% corresponding to 62.2 W at the MPC output (see Methods for details). The efficiency can be improved by reducing the number of optical windows or by improved anti-reflection coatings.

The input spectrum of the laser sent into the MPC, and the corresponding output spectra after the MPC for optimized pulse shaper settings, which yield spectral shifts to 999 nm and 1,062 nm, are shown in Fig. 2b. The corresponding filtered spectra obtained using spectrally tunable dichroic mirrors are shown in Fig. 2c. After spectral filtering, we reach 66.7% (41.5 W) and 63% (39.2 W) of the optical power transmitted

through the MPC centred at 1,062 nm and 999 nm, respectively. We observed that the achievable efficiency depends critically on the MPC mirror performance and deteriorates with increasing nonlinear phase acquired in the CPA amplifier chain after the pulse shaper. A large nonlinear phase reduces the pulse-shaping performance at the CPA output.

Contrary to SPM-based spectral broadening in an MPC typically yielding a positively chirped pulse at the MPC output, we observe that the frequency-shifted pulses exhibit a small negative chirp. After spectral filtering, the wavelength-shifted pulses can be compressed to durations of 106 fs (1,062 nm) and 92 fs (999 nm) by passing 119 mm and 100 nm fused silica, respectively. The temporal reconstruction from second harmonic frequency-resolved optical gating (FROG) measurements of the laser output pulses at 1,030 nm, as well as the spectrally shifted and compressed pulses, are displayed in Fig. 2d, revealing excellent temporal pulse quality. It should be noted that the temporal output pulse shape after the MPC is approximately identical to the input pulse shape. This is ensured by the dispersion-compensating MPC design; however, after the spectral filter and compressor, the pulse profile changes to a Gaussian shape. We also verify the spatial beam quality after spectral shifting. With an input beam quality parameter  $M^2 = 1.2 \times 1.4$ , we obtain output beam parameters of  $M^2 = 1.2 \times 1.3$  at 1,062 nm and  $1.3 \times 1.6$  at 999 nm.

Encouraged by the great temporal pulse quality revealed by FROG measurements, we explore the temporal contrast of the frequency-shifted pulses. As in the radiofrequency domain, in which

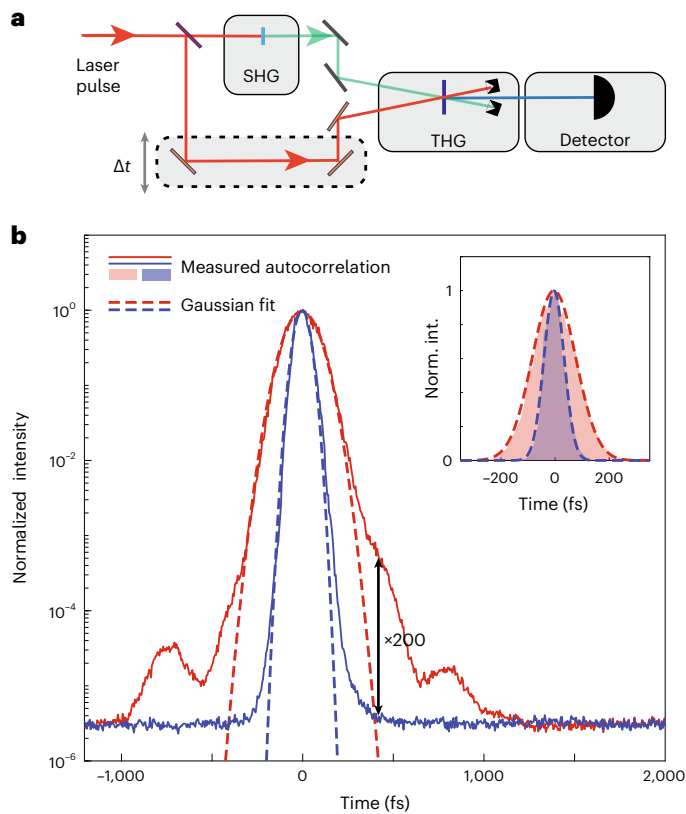


**Fig. 3 | Temporal contrast characterization.** **a**, Schematic of the third-order autocorrelator used to measure the temporal contrast of the frequency-shifted pulses. **b**, Measured autocorrelation signals (solid lines) for the laser output at 1,030 nm (red) and spectrally shifted and filtered pulse at 1,062 nm (blue). Gaussian curves (dashed lines) are fitted to the autocorrelation data. The inset in **b** shows the corresponding signals in linear scale.

frequency-shifting methods are employed for signal-to-noise reduction<sup>26</sup>, nonlinear frequency shifting of optical signals can enhance the temporal pulse contrast<sup>27</sup>. To verify this, we measure the third-order autocorrelation of the pulse using the set-up shown in Fig. 3a. The intensity cross-correlation between an input pulse and its second harmonic for an input centre wavelength at 1,033 nm, and the wavelength-shifted and spectrally filtered pulse at 1,062 nm, are shown in Fig. 3b. We find that the temporal pedestals are reduced by a factor of up to at least 200, limited by the dynamic range of our detector. By contrast to typical post-compressed pulses exhibiting temporal pre- and post-pulses<sup>28</sup>, the frequency-shifted pulses have a nearly perfect Gaussian shape over a large dynamic range.

Another particularly important property for frequency comb lasers is coherence. Coherence properties of spectrally broadened laser pulses generated, for example, via super-continuum generation in highly nonlinear fibres and typically operated at an average power of a few milliwatts, have been explored in detail<sup>29</sup>. Here we study the coherence characteristics of a spectrally shifted high-power laser. We lock a nonlinearly amplified portion of our frequency comb oscillator to a stable continuous-wave reference laser, choosing a lock-offset frequency of 20 MHz between both lasers. The continuous-wave laser has a linewidth of around 1 kHz and a wavelength of 1,064 nm. The schematic of the locking scheme is shown in Fig. 4a. The continuous-wave laser is further used to produce a heterodyne beat note with the frequency-shifted output after the MPC, centred at 1,062 nm. The measured beat note location at 20 MHz resembles the chosen lock-offset, thus confirming preservation of the carrier-envelope offset

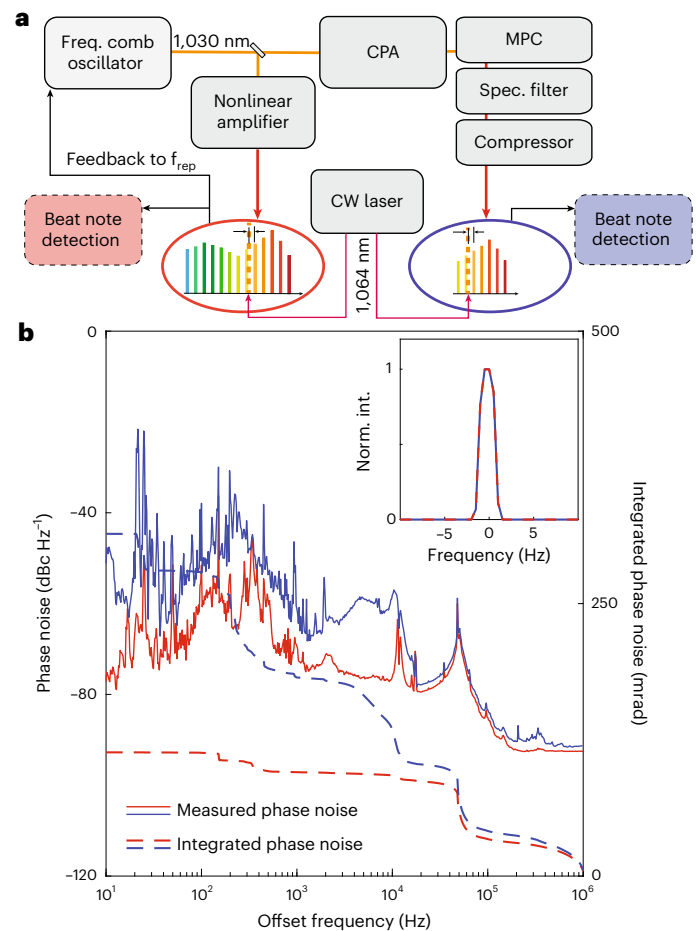


**Fig. 4 | Coherence demonstration.** **a**, Schematic of the set-up used to characterize the coherence properties of the frequency-shifted high-power frequency comb. A nonlinearly amplified portion of the oscillator output is used for stabilization to a continuous-wave reference laser at 1,064 nm via feedback to the repetition rate  $f_{\text{rep}}$  of the comb. The same continuous-wave laser is used to produce a coherent beat note with the frequency-shifted laser. **b**, Measured in-loop phase noise (red solid line), and beat note phase noise of the spectrally shifted laser with the continuous-wave laser (blue solid line) displayed together with the integrated phase noise (dashed lines). The inset in **b** shows the corresponding beat notes measured on a radiofrequency spectrum analyser with a resolution bandwidth of 1.5 Hz.

frequency in the Serrodyne shifting process. Figure 4b displays the measured in-loop phase noise of the referenced laser together with the phase-noise detected after frequency-shifting. The inset shows the corresponding beat notes, indicating hertz-level linewidth support. We find that the integrated phase noise (10 Hz to 1 MHz) of the laser and spectrally shifted output amount to 113.5 mrad and 314.1 mrad, respectively, corresponding to about 99% and 90% of the power contained in the carrier<sup>30</sup>. This result demonstrates excellent coherence properties of our method, setting an upper bound for a possible coherence degradation due to the shifting process. Furthermore, due to amplitude-to-phase noise coupling induced by the nonlinearity in the MPC, a low output phase noise of the shifted output implies a low input amplitude noise.

In this work we have introduced a versatile wavelength-tuning method for ultrashort lasers, supporting excellent temporal pulse quality and great coherence characteristics. We experimentally demonstrate our method shifting femtosecond laser pulses from 1,030 nm to 999 nm and 1,062 nm, limited in shifting range mainly by the MPC

mirror bandwidth. Using numerical simulations, we show that the method can be extended to larger spectral shifts, provided that sufficiently broadband mirrors are employed.

Our concept provides great prospects for the versatile implementation of wavelength-tunable laser sources covering large parameter ranges as it is based on nonlinear MPCs that have been exhibited at pulse energies covering a few microjoules to 100 mJ, average powers of up to 1 kW, and pulse durations ranging from picoseconds to few optical cycles<sup>14</sup>. In particular, when used with high-power ytterbium lasers and high-pulse-energy MPCs<sup>14,31</sup>, wavelength-tunable lasers with terawatt-scale peak powers and kilowatts of average power can be realized<sup>13,32</sup>. The method thus promises an effective route for laser platforms to provide high average powers, shot pulse durations and wavelength-tunability in a single unit, thus combining complementary advantages previously learned from different laser architectures. Depending on the laser platform, pulse-shaping limitations that might arise in the amplifier chain when using a pulse shaper in the laser front-end can be circumvented by direct phase shaping of the amplified laser pulses. A high-power phase shaper can be implemented, for example, via a phase mask or deformable mirror in the CPA compressor<sup>33</sup>.

Serrodyne frequency-shifted femtosecond lasers thus have the potential to boost various applications ranging from remote sensing over frequency comb spectroscopy to multiphoton microscopy. Furthermore, nonlinear spectroscopy methods and applications that use secondary laser-driven high harmonic sources as, for example, attosecond science could greatly benefit from continuously tunable extreme ultraviolet sources driven by wavelength-tunable lasers. Furthermore, applications demanding highest peak or average power lasers such as laser plasma acceleration<sup>34</sup> or semiconductor chip production<sup>3</sup>, which were so far constrained to a single or very few operation points in the electromagnetic spectrum, will benefit from novel optimization opportunities. Finally, the here-presented ultrafast serrodyne optical frequency-shifting scheme can prospectively be extended to other MPC input pulse shapes optimized for targeted output spectra, including spectra exhibiting, for example, two separated peaks or a defined output bandwidth. Likewise, an optimization target can be defined in the time domain, reached—optionally after further spectral shaping—at the MPC output.

## Online content

Any methods, additional references, Nature Portfolio reporting summaries, source data, extended data, supplementary information, acknowledgements, peer review information; details of author contributions and competing interests; and statements of data and code availability are available at <https://doi.org/10.1038/s41566-022-01121-9>.

## References

- Corkum, P. B. & Krausz, F. Attosecond science. *Nat. Phys.* **3**, 381–387 (2007).
- Antognini, A. et al. Proton structure from the measurement of 2s–2p transition frequencies of muonic hydrogen. *Science* **339**, 417–420 (2013).
- Versolato, O. O., Sheil, J., Witte, S., Ubachs, W. & Hoekstra, R. Microdroplet-tin plasma sources of EUV radiation driven by solid-state-lasers (topical review). *J. Opt.* **24**, 054014 (2022).
- Stolen, R. H., Ippen, E. P. & Tynes, A. R. Raman oscillation in glass optical waveguide. *Appl. Phys. Lett.* **20**, 62–64 (1972).
- Vanvincq, O., Kudlinski, A., Bétourné, A., Quiquempois, Y. & Bouwmans, G. Extreme deceleration of the soliton self-frequency shift by the third-order dispersion in solid core photonic bandgap fibers. *J. Opt. Soc. Am. B* **27**, 2328–2335 (2010).
- Mitschke, F. M. & Mollenauer, L. F. Discovery of the soliton self-frequency shift. *Opt. Lett.* **11**, 659–661 (1986).
- Gordon, J. P. Theory of the soliton self-frequency shift. *Opt. Lett.* **11**, 662–664 (1986).
- Wai, P. K. A., Menyuk, C. R., Lee, Y. C. & Chen, H. H. Nonlinear pulse propagation in the neighborhood of the zero-dispersion wavelength of monomode optical fibers. *Opt. Lett.* **11**, 464–466 (1986).
- Travers, J. C., Grigorova, T. F., Brahms, C. & Belli, F. High-energy pulse self-compression and ultraviolet generation through soliton dynamics in hollow capillary fibres. *Nat. Photon.* **13**, 547–554 (2019).
- Beetar, J. E. et al. Multioctave supercontinuum generation and frequency conversion based on rotational nonlinearity. *Sci. Adv.* **6**, eabb5375 (2020).
- Tyumenov, R., Hammer, J., Joly, N. Y., Russell, P. S. J. & Novoa, D. Tunable and state-preserving frequency conversion of single photons in hydrogen. *Science* **376**, 621–624 (2022).
- Fattahi, H. et al. Third-generation femtosecond technology. *Optica* **1**, 45–63 (2014).
- Grebing, C., Müller, M., Buldt, J., Stark, H. & Limpert, J. Kilowatt-average-power compression of millijoule pulses in a gas-filled multi-pass cell. *Opt. Lett.* **45**, 6250–6253 (2020).
- Viotti, A.-L. et al. Multi-pass cells for post-compression of ultrashort laser pulses. *Optica* **9**, 197–216 (2022).
- Winnall, S., Lindsay, A. & Knight, G. A wide-band microwave photonic phase and frequency shifter. *IEEE Trans. Microw. Theory Tech* **45**, 1003–1006 (1997).
- McDermitt, C. & Bucholtz, F. Rf frequency shifting via optically switched dual-channel pzt fiber stretchers. *IEEE Trans. Microw. Theory Tech.* **53**, 3782–3787 (2005).
- Houtz, R., Chan, C. & Müller, H. Wideband, efficient optical serrodyne frequency shifting with a phase modulator and a nonlinear transmission line. *Opt. Express* **17**, 19235–19240 (2009).
- Johnson, D. M. S., Hogan, J. M., Chiow, S. W. & Kasevich, M. A. Broadband optical serrodyne frequency shifting. *Opt. Lett.* **35**, 745–747 (2010).
- Lee, K. F. & Kanter, G. S. All-optical serrodyne frequency shifter. *Opt. Express* **29**, 26608–26617 (2021).
- Lauerhmann, M. et al. Integrated optical frequency shifter in silicon-organic hybrid (SOH) technology. *Opt. Express* **24**, 11694–11707 (2016).
- Kohlhaas, R. et al. Robust laser frequency stabilization by serrodyne modulation. *Opt. Lett.* **37**, 1005–1007 (2012).
- Cumming, R. C. The serrodyne frequency translator. *Proc. IRE* **45**, 175–186 (1957).
- Schulte, J., Sartorius, T., Weitenberg, J., Vernaleken, A. & Russbuedt, P. Nonlinear pulse compression in a multi-pass cell. *Opt. Lett.* **41**, 4511–4514 (2016).
- Weitenberg, J. et al. Multi-pass-cell-based nonlinear pulse compression to 115 fs at 7.5 μJ pulse energy and 300 W average power. *Opt. Express* **25**, 20502–20510 (2017).
- Heyl, C. M. et al. Wavelength conversion apparatus and method for spectrally converting laser pulses, and laser source apparatus including the wavelength conversion apparatus. *Eur. Pat.* EP22171982 (2022).
- Johnson, L. & Cox, C. Serrodyne optical frequency translation with high sideband suppression. *J. Light. Technol.* **6**, 109–112 (1988).
- Buldt, J. et al. Temporal contrast enhancement of energetic laser pulses by filtered self-phase-modulation-broadened spectra. *Opt. Lett.* **42**, 3761–3764 (2017).
- Viotti, A.-L. et al. 60 fs, 1030nm FEL pump-probe laser based on a multi-pass post-compressed Yb:YAG source. *J. Synchrotron Radiat.* **28**, 36–43 (2021).
- Schibli, T. et al. Optical frequency comb with sub-millihertz linewidth and more than 10 W average power. *Nat. Photon.* **2**, 355–259 (2008).

30. Arimondo, E., Phillips, W. & Strumia, F. *Laser Manipulation of Atoms and Ions* (Elsevier, 1993).
31. Heyl, C. M. et al. High-energy bow tie multi-pass cells for nonlinear spectral broadening applications. *J. Phys. Photon.* **4**, 014002 (2022).
32. Stark, H., Buldt, J., Müller, M., Klenke, A. & Limpert, J. 1 kW, 10 mJ, 120 fs Coherently combined fiber CPA laser system. *Opt. Lett.* **46**, 969–972 (2021).
33. Zeek, E. et al. Pulse compression by use of deformable mirrors. *Opt. Lett.* **24**, 493–495 (1999).
34. Albert, F. et al. 2020 roadmap on plasma accelerators. *New J. Phys.* **23**, 031101 (2021).

**Publisher's note** Springer Nature remains neutral with regard to jurisdictional claims in published maps and institutional affiliations.

**Open Access** This article is licensed under a Creative Commons Attribution 4.0 International License, which permits use, sharing, adaptation, distribution and reproduction in any medium or format, as long as you give appropriate credit to the original author(s) and the source, provide a link to the Creative Commons license, and indicate if changes were made. The images or other third party material in this article are included in the article's Creative Commons license, unless indicated otherwise in a credit line to the material. If material is not included in the article's Creative Commons license and your intended use is not permitted by statutory regulation or exceeds the permitted use, you will need to obtain permission directly from the copyright holder. To view a copy of this license, visit <http://creativecommons.org/licenses/by/4.0/>.

© The Author(s) 2022

## Methods

### Laser and multi-pass cell

The ytterbium laser we used for frequency shifting consists of a nonlinear amplifying loop mirror oscillator<sup>35</sup> with an average output power of 12 mW, a pulse duration of 150 fs and a repetition rate of 65 Mhz. This oscillator is first amplified to 300 mW in a fibre amplifier. A 165 m polarization-maintaining fibre then stretches the pulses to 120 ps. The stretched pulses are sent through a pulse shaper, which consists of a programmable spatial light modulator. The input power into the spatial light modulator is 300 mW, which results in an output power of 82 mW. Afterwards, the pulses are amplified in a double-clad ytterbium-doped fibre, followed by a rod-type amplifier delivering about 100 W output power. Finally, using a grating compressor, the pulses are compressed to 205 fs, with a Fourier limit of 190 fs at a wavelength centred at 1,033 nm. At the input to the MPC, an average power of 76 W is reached. The nonlinear phase accumulated in the fibre sections between the wave shaper and laser output was estimated using numerical simulations resulting in 3.88 rad. It should be noted that we observed no substantial dependence of the amplifier performance on the pulse shaper settings when applied for phase shaping only.

The MPC consists of two concave mirrors with radii of curvature 100 mm, separated by a distance of 187 mm. The mirrors are coated with a dispersive coating of  $-200 \text{ fs}^2$  matched to 10.5 mm fused silica. The nonlinear medium in this MPC consists of five anti-reflection-coated solid fused silica windows. One window with a thickness of 6.35 mm is placed at the focus; four windows with a thickness of 1 mm are placed at a distance of about 20 mm and 40 mm from the focus. The MPC accommodates 32 round trips.

### Simulations and optimization

The simulations for the spectral-shifting results presented in Fig. 1b were performed by solving the forward Maxwell equation<sup>36</sup>. The considered mirror characteristics are taken from commercially available dielectric mirrors providing dispersion properties matched to 2 mm fused silica over a wide spectral range upon reflection at a mirror pair. To provide two mirror reflections in between consecutive passes through the nonlinear medium, an MPC consisting of four mirrors is required. The centre wavelength of 800 nm was chosen based on available broadband coatings. The nonlinear phase accumulated per pass (about 1.7 rad) lies within the range enabling multi-plate based MPC spectral broadening while supporting excellent spatial beam quality<sup>37</sup>.

To optimize the phase required for spectral shifting, we employ a numerical library with support for automatic differentiation<sup>38</sup> and an optimization library originally developed to train neural networks (Optax<sup>39</sup>). We start the optimization process by launching a pulse with a spectral phase representing a good guess for a temporally asymmetric pulse form approaching a saw-tooth shape (transform-limited pulse duration: 40 fs, Gaussian spectral amplitude) into the MPC. The phase is iteratively optimized using Optax. This allows a relatively large parameter space to be optimized efficiently. A careful manual adaption of suitable target functions allows us to mitigate termination of the optimization process in local minima, a typical issue for gradient descent methods.

In our numerical simulations and experimental implementation, we have only used spectral phase-shaping methods; however, the temporal-shaping performance can be improved by adding amplitude shaping.

### Third-order autocorrelator

A third-order autocorrelator was built for high-dynamic range temporal pulse characterization; the set-up is shown in Fig. 3a. First, infrared laser pulses with a pulse energy of about 0.5  $\mu\text{J}$  are split into two arms of an interferometer. In the first arm, a second harmonic signal is generated using a type-I barium borate crystal with 50  $\mu\text{m}$  thickness. Then the second harmonic pulses are combined non-collinearly with the second

interferometer arm and focused into a type-II barium borate crystal with 50  $\mu\text{m}$  thickness to generate a third harmonic signal. The temporal delay between the fundamental and the second harmonic beam is adjusted using a motorized delay stage. The third harmonic signal is then detected with a biased ultraviolet-enhanced silicon photo diode (UV-001DQ from OSI Optoelectronics). The signal is amplified with the help of a transimpedance amplifier (DHPCA-100 from FEMTO). We have verified the linearity of the photodiode to detect the third harmonic signal over the full dynamic range displayed in Fig. 3b.

### Data availability

The datasets that support the plots within this paper are available from the authors on reasonable request.

### Code availability

The custom code used for the simulation of the frequency-shifting process is available from the authors on reasonable request.

## References

35. Ma, Y. et al. Compact, all-PM fiber integrated and alignment-free ultrafast yb: fiber NALM laser with sub-femtosecond timing jitter. *J. Light. Technol.* **39**, 4431–4438 (2021).
36. Couairon, A. et al. Practitioner's guide to laser pulse propagation models and simulation. *The Eur. Phys. J. Special Top.* **199**, 5–76 (2011).
37. Seidel, M. et al. Ultrafast MHz-rate burst-mode pump-probe laser for the FLASH FEL facility based on nonlinear compression of ps-level pulses from an yb-amplifier chain. *Laser Photon. Rev.* **16**, 2100268 (2022).
38. Bradbury, J. et al. *JAX: Composable Transformations of Python + NumPy Programs* (Github, 2018).
39. Hessel, M. et al. *Optax: Composable Gradient Transformation and Optimisation, In Jax!* (Github, 2020).

## Acknowledgements

We acknowledge DESY (Hamburg, Germany) and Helmholtz-Institute Jena (Germany), and members of the Helmholtz Association HGF for support and/or the provision of experimental facilities. H. T. acknowledges support from the IVF project InternLabs-0011(HIR3X).

## Author contributions

P.B., H.T., S.S., M.F. and S.A. conducted the experiments, C.M.H. conceived the initial idea, P.B. verified the initial idea with simulations and conducted all further simulations with H.T. C.M.H. and I.H. supervised the project, and all authors contributed to the writing of the manuscript.

## Funding

Open access funding provided by Deutsches Elektronen-Synchrotron (DESY).

## Competing interests

The authors declare no competing interests.

## Additional information

**Correspondence and requests for materials** should be addressed to Christoph M. Heyl.

**Peer review information** *Nature Photonics* thanks Almantas Galvanauskas and the other, anonymous, reviewer(s) for their contribution to the peer review of this work.

**Reprints and permissions information** is available at [www.nature.com/reprints](http://www.nature.com/reprints).